Soft Matter

PAPER

View Article Online
View Journal | View Issue

Cite this: *Soft Matter*, 2017, 13, 658

Phase transition and aggregation behaviour of an UCST-type copolymer poly(acrylamide-*co*-acrylonitrile) in water: effect of acrylonitrile content, concentration in solution, copolymer chain length and presence of electrolyte†

Asad Asadujjaman,[a] Ben Kent[b] and Annabelle Bertin*[ac]

Received 5th October 2016,
Accepted 28th November 2016

DOI: 10.1039/c6sm02262f

www.rsc.org/softmatter

An UCST-type copolymer of acrylamide (AAm) and acrylonitrile (AN) (poly(AAm-*co*-AN)) was prepared by reversible addition fragmentation chain transfer (RAFT) polymerization and its temperature-induced phase transition and aggregation behaviour studied by turbidimetry, static and dynamic light scattering, small angle neutron scattering (SANS) and cryo-transmission electron microscopy (cryo-TEM) measurements. The phase transition temperature was found to increase with increasing AN content in the copolymer, concentration of the solutions and copolymer chain length. A significant effect was observed onto the phase transition temperature by addition of different electrolytes into the copolymer solution. The copolymer chains were aggregated below the phase transition temperature and disaggregated above it. The size of the aggregates increases with increasing AN contents and concentration of the copolymer solutions below the phase transition temperature. The copolymer chains were expanded and weekly associated in solution above the phase transition temperature. A model is proposed to explain such association–aggregation behaviour of poly(AAm-*co*-AN) copolymers depending on AN contents and concentration of the copolymer solutions as a function of temperature.

1 Introduction

The physical properties of smart polymeric materials change according to environmental factors, such as temperature, pH, light, electric and magnetic fields and ionic strength.[1] It is the thermoresponsive polymers ability to change their physical properties in response to change to the surrounding temperature that makes them the most interesting materials within this group of smart polymeric materials. This is especially the case in areas such as temperature-triggered drug delivery, diagnostics, tissue engineering, bio-separation, thermally switchable optical devices, and in sensory applications.[1–5] Thermoresponsive polymers can exhibit a lower critical solution temperature (LCST)[6] and/or an upper critical solution temperature (UCST).[7,8]

There has been a recent increased interest in UCST polymers. However, to date, only few polymers exhibiting a UCST in water within a relevant temperature range (0 to 100 °C), have been reported, *i.e.* phase separate from solution upon cooling.[9–11] In addition, UCST type polymers based on ionic interactions such as polybetaines,[12–15] are difficult to use under physiological conditions (*i.e.* in the presence of salts *etc.*), which significantly restricts their potential applications. Therefore, non-ionic based UCST polymers with sharp and robust phase transition in physiological conditions are urgently needed in order to extend the range of applications of this class of polymers.

Non-ionic based UCST polymers rely on hydrogen bonding between polymer side groups for the phase transition. With increasing temperature, the hydrogen bonds between polymer side groups are broken in an endothermic process and replaced by hydrogen bonds with water molecules in an exothermic process.[16] Examples are poly(*N*-acryloylglycinamide) (PNAGA), first synthesized by Haas and Schuler,[17] and poly(uracilacrylate), synthesized by Brahme and Smith.[18] These polymers show a UCST in a relevant temperature range (5–60 °C) in aqueous solutions.[10] The UCST behaviour of PNAGA in both pure water and also in electrolyte solution was first reported by Agarwal *et al.*[19] Since then, PNAGA has been studied more extensively

[a] *Federal Institute for Materials Research and Testing (BAM), Unter den Eichen 87, 12205 Berlin, Germany. E-mail: annabelle.bertin@bam.de*
[b] *Helmholtz-Zentrum Berlin (HZB), Hanhn-Meitner-Platz 1, 14109 Berlin, Germany*
[c] *Freie Universität Berlin, Institute of Chemistry and Biochemistry–Organic Chemistry, Takustr. 3, 14195 Berlin, Germany*

† Electronic supplementary information (ESI) available: Summary of the synthesis [Table S1], ^{1}H-NMR spectrum [Fig. S2], ATR-FTIR spectrum [Fig. S3], GPC data [Fig. S4], ATR-FTIR calibration curves [Fig. S5], DLS curves [Fig. S6] and d*n*/d*c* curve [Fig. S7]. See DOI: 10.1039/c6sm02262f

than the other non-ionic UCST polymers. However, it has been discovered that the presence of a trace amount of ionic groups during polymerization significantly affects the phase transition or even suppresses its UCST behaviour. Moreover, PNAGA and its derivatives display a significant hysteresis[20] and exhibit a slow phase transition,[19] preventing their use in many applications where sharp and fast transitions are required. Another example of non-ionic UCST polymer is acrylamide based poly(methylacrylamide) (PMAm).[21] However, the UCST behaviour of PMAm is also affected by the presence of ionic groups during synthesis. Acrylamide based copolymers, for example interpenetrating networks and cross-linked gels of poly(acrylamide-*co*-acrylic acid), exhibit UCST behaviour,[22–24] though non-cross-linked copolymers have not been reported yet to show UCST. It is also known that the homopolymer poly(acrylamide) is completely soluble in pure water.

There is growing interest for copolymers based on acrylamide (AAm) and acrylonitrile (AN) (poly(AAm-*co*-AN)) first reported by Seuring and Agarwal,[21] in the field of non-ionic based UCST polymers. Poly(AAm-*co*-AN) copolymers show a sharp and reversible UCST phase transition in aqueous and electrolyte solutions. The phase transition temperature of this copolymer can be adjusted or tuned by varying the composition of the copolymer and the concentration of the solution.[21] Additionally, the UCST type poly(AAm-*co*-AN) based derivatives show potential applications as microactuators[25] and drug delivery systems.[26] Very recently Pineda-Contreras *et al.*[27] investigated the pH dependent thermoresponsive behaviour of the poly(AAm-*co*-AN) in aqueous media. The results showed a high tolerance of UCST properties of poly(AAm-*co*-AN) under extreme acidic conditions. However, the thermoresponsivity is significantly affected during hydrolysis in basic condition. The report of Hou *et al.*[28] describes the effects of solvent isotopes on the UCST behaviour of poly(AAm-*co*-AN), as well as the interaction mechanism between the copolymer chains and the solvent molecules. It was shown that the phase transition temperature is almost 10 °C higher in D_2O than in H_2O solution at the same concentration. Indeed, relatively ''free'' C═O groups in H_2O solutions are believed to be responsible for lowering the UCST in H_2O compared to D_2O solution. However, the aggregation behaviour of this thermoresponsive polymeric systems above and below the UCST has not been yet described. The pH-induced water solubility switch of poly(AAm-*co*-AN) and its copolymer with either acrylic acid (AAc) or 4-vinylpyridine (4VP) was investigated by Zhang *et al.*[29] The phase transition temperature of poly(AAm-*co*-AN) changed slightly (around 2 °C) by increasing pH from 3.0 to 10.0. However, a large drop in the phase transition temperature from 50 °C to 26 °C was observed for the poly(AAm-*co*-AN-*co*-AAc) with increasing pH from 2 to 3.5. Moreover, the phase transition temperature of poly(AAm-*co*-AN-*co*-4VP) decreased from 75 °C to 15 °C by reducing pH from 4.75 to 3.0. Zhao *et al.*[30] prepared three different types of block copolymers using poly(AAm-*co*-AN) copolymer coupled with either hydrophobic polystyrene, hydrophilic poly(dimethyl acrylamide) or poly(*N*,*N*-dimethylaminoethylmethacrylate) presenting a phase transition temperature around 48, 14 and 20 °C respectively. The authors investigated the thermoresponsivity and aggregation behaviour of the obtained block copolymers and found reversible dispersion/aggregation of micelles, dissolution/formation of micelles, and reversal of the micelle core and corona in either water or buffer solution under varying the temperatures from 5 to 70 °C. In addition, Käfer *et al.*[31] showed that the UCST-type single phase behaviour of poly(AAm-*co*-AN) can be extended to a double responsive behaviour, *i.e.* LCST–UCST-type in aqueous media by introduction of a poly(ethylene glycol) (PEG) block. The morphology of the poly(AAm-*co*-AN)-PEG block copolymer changes from micelles to agglomerates by increasing the surroundings temperature.

In this report, poly(AAm-*co*-AN) copolymers with different AN fractions were synthesized *via* reversible addition–fragmentation chain transfer (RAFT) polymerization. The temperature-induced phase transition of poly(AAm-*co*-AN) and the nature of its aggregation behaviour was investigated around the phase transition temperature in pure water and in the presence of electrolytes by turbidimetry, static and dynamic light scattering (SLS and DLS), small angle neutron scattering (SANS), and cryo-transmission electron microscopy (cryo-TEM) measurements. We describe the aggregation behaviour of poly(AAm-*co*-AN) above and below its phase transition temperature as the size of thermoresponsive polymeric systems is of prime importance for biomedical applications (as size dependent processes take place in the body)[32] and is linked to the optical properties of a material that matter in materials science.[33] It was observed that poly(AAm-*co*-AN) copolymer solutions show a UCST-type phase transition behaviour when the hydrophilic–lipophilic balance of the copolymer was adequate. The phase transition temperature was found to increase with increasing AN fraction, concentration of the copolymer solutions and copolymer chain length. The phase transition temperature was also influenced by the addition of different electrolytes into the copolymer solutions. Below the phase transition temperature of poly(AAm-*co*-AN), the copolymer chains were collapsed and aggregated. The size of the aggregates was found to be larger with increasing AN fraction or solution concentration. Above the phase transition temperature of poly(AAm-*co*-AN), the copolymer chains were in some cases found to be slightly associated and the extent of this association was related to the AN content in the copolymer. Based on the observed results, we propose a model for the phase transition and aggregation behaviour of poly(AAm-*co*-AN) depending on the AN fraction in the copolymer and the concentration of the solution.

2 Experimental

2.1 Materials

Acrylamide (Sigma Aldrich, >99%, electrophoresis grade), acrylonitrile (Fisher Scientific, >99%), 2,2′-azobis-(2,4-dimethylvaleronitrile) (ABDV) (Wako, 95%) and 4-cyano-4-[(dodecylsulfanylthiocarbonyl)sulfanyl]pentanoic acid (TTC) (Sigma Aldrich, 97%) were used as received. Dimethyl sulfoxide (DMSO) (Merck, >99%), methanol (Fischer Scientific, >99.9%) and other solvents were used without further purification. Ultrapure water was obtained from Sartorius system.

2.1.1 Synthesis of poly(AAm-*co*-AN) with varying AN contents. As an example, the polymerization with 0.225 mol% of AN in the feed for a desired degree of polymerization of 500 was conducted as follows: prior to the reaction DMSO was degassed by three freeze–pump–thaw cycles. Acrylamide (4.1 g, 57.6 mmol), acrylonitrile (1.1 mL, 16.7 mmol), ABDV initiator (4.0 mg, 0.014 mmol) and TTC (60.0 mg, 0.14 mmol) were dissolved in degassed DMSO (25 mL) in a 100 mL three-necked flask. Afterwards the reaction mixture was heated to 55 °C for 24 h. The reaction was halted by cooling the flask in cold water and opening it to air. The product was obtained from precipitation in methanol and dialyzed against water (MWCO 3000) at 65 °C for 8 h. Finally, the product was freeze dried and obtained as slight yellowish solid product (3.4 g, yield 65%). All other reactions were carried out similarly. More details are given in Table S1 (ESI†). ^{1}H-NMR (400 MHz, DMSO-d_6) δ (ppm) = 0.87 (–CH_3–), 1.29–1.9 (–CH_2–), 2.0–2.6 (–CH–$CONH_2$), 2.3–3.0 (–CH–CN), 6.9 (–NH_2) (see Fig. S2 (ESI†)). FTIR (ATR-IR): ν (cm^{-1}) = 3650–3050 (mb, NH), 3000–2850 (w, CH), 2242 (w, CN), 1659 (vs, CO) (Fig. S4 (ESI†)).

2.2 Analytical techniques

2.2.1 NMR measurements. The ^{1}H-NMR spectra were recorded with a Brucker Biospin AC-400 device. The indicated chemical shift is relative to the signal of the deuterated solvent as the internal standard ($(CD_3)_2SO$).

2.2.2 ATR-FTIR spectroscopy. ATR-FTIR spectra were recorded by using Nicolet 8700 Thermo Scientific spectrometer with smart orbit diamond cryo 2012 equipped with an IR light source, a MCT/A detector in the range of 550 to 4000 cm^{-1}. The measurements were performed using Omnic version 7.3 software (Thermo Electron Corporation) and each spectrum is the average 32 scans with a measurement time of 32 s and a resolution of 4000 cm^{-1} using auto baseline correction.

2.2.3 Gel permeation chromatography (GPC). GPC measurements were performed using a PSS-GRAM 7μ VS + 100 + 1000 column with *N*-methylpyrrolidone (NMP) plus 0.5 g L^{-1} of LiBr as an eluent at a flow rate of 0.8 mL min^{-1} at 70 °C and calibrated with polystyrene as standard in the molecular weight range of 600 to 2.0 × 10^6 g mol^{-1}.

2.2.4 Turbidimetry measurements. Turbidimetry measurements were conducted using a turbidimetric photometer TP1 (Elmar Tepper, Germany) at a temperature gradient of 1 °C min^{-1}. The measurements were performed using hyperterminal software at wavelength of 670 nm in the heating and cooling cycles. The raw data was normalized and then transformed to transmission.

2.2.5 Dynamic light scattering (DLS). DLS measurements were carried out on ALV/CGS-3 compact goniometer connected with LSE-5004 digital correlator (ALV/LSE 5004 Light Scattering Electronics and Multiple Tau digital Correlator). A 22 mW He–Ne laser (wavelength 632.6 nm) was used as a light source. The measurements were performed using the ALV-5000VE/EPP software as a function of temperature. At each measurement temperature the samples were equilibrated 120 s and the temperature increment was 2 °C. The temperature gradient was 0.5 °C min^{-1} controlled by Julabo thermobath. Hydrodynamic radius (R_h) of the samples was calculated at 90° angle using Cumulant method.[34]

2.2.6 Static light scattering (SLS). SLS measurements were carried out on ALV/CGS-3 compact goniometer connected with LSE-5004 digital with a 22 mW He–Ne laser as light source. The weight average molar mass (M_w), time dependent average scattering intensity $R(\theta)$ at θ angle, the second viral coefficient (A_2) and the scattering vector q are related as:[35]

$$\frac{Kc}{R(\theta)} = \frac{1}{M_w} + \left(1 + \frac{R_g^2 q^2}{3}\right) + 2A_2C \quad (1)$$

where $K = 4\pi n^2(dn/dc)^2/(N_A\lambda_0^4)$ and $q = (4\pi n/\lambda)\sin(\theta/2)$, with N_A, n, λ_0 and c are the Avogadro's constant, refractive index, wavelength in vacuum and the sample concentration in g mL^{-1}, respectively. The specific refractive index increment of the solution (dn/dc) was measured with dndc 2010 with 620 nm light source (PSS, Mainz, Germany). The measured refractive index increment (dn/dc) of poly(AAm-*co*-AN) is ~0.16 mL g^{-1} in water (Fig. S7 (ESI†)). To determine the weight average apparent molecular weight ($M_{w,app}$) of the copolymer solution, eqn (1) was expressed as:

$$\frac{Kc}{R(\theta \to 0)} = \frac{1}{M_{w,app}}. \quad (2)$$

The $Kc/R(\theta \to 0)$ can be obtained by extrapolating the $Kc/R(\theta)$ *vs.* q^2 plot (Zimm plot) to zero scattering angle. The measurements were done at scattering angles between 26 and 158°. The sample was equilibrated for 2 min at each temperature.

2.2.7 Small angle neutron scattering (SANS). SANS measurements were performed using the V16 instrument[36] at Helmholtz-Zentrum Berlin (HZB). Data was recorded at two sample-detector distances: 1.7 m with neutron wavelength 1.8–3.8 Å, and 11 m with neutron wavelength 1.6–9.2 Å. Samples were prepared in D_2O and measured at 25 °C and 60 °C. Samples were equilibrated at measurement temperature for least 30 min prior to measurement. Data was corrected for transmission, background detector counts, empty cell scattering, and detector efficiency, then scaled to absolute intensity using a 1 mm H_2O measurement. Data from both configurations was radially averaged and combined to give a total q range of 0.007–0.5 $Å^{-1}$.

2.2.8 Cryogenic transmission electron microscopy (cryo-TEM). A droplet (5 μL) of the sample solution was placed on hydrophilized (plasma treatment using a BALTEC MED 020 device (Leica Microsystems, Wetzlar, Germany)), perforated carbon filmed grids (Quantifoil Micro Tools GmbH, Jena, Germany). The excess fluid was removed by blotting to create an ultra-thin layer (typical thickness of 200–300 nm) of the solution, which spans the holes of the support film. The prepared samples were immediately vitrified by propelling the grids into liquid ethane at its freezing point (−184 °C). The vitrified sample grids were transferred under liquid nitrogen by the use of a Gatan (Pleasanton, CA, USA) cryo-holder (Model 626) into a Tecnai F20 TEM (FEI company, Oregon, USA) equipped with FEG and operated at 160 kV acceleration voltage. Microscopy was carried out at −175 °C sample temperature using the microscope's low dose protocol at calibrated primary magnifications of 5k and 29k. The defocus was set to be 9.81 μm (29k). Images were recorded by the use of a 4k-Eagle CCD camera (FEI Company, Oregon, USA) at 2k resolution (binning 2).

3 Results and discussion

3.1 Synthesis

Poly(AAm-*co*-AN) copolymers were prepared *via* controlled RAFT polymerization and by varying the AN feed for a given molecular weight ($\sim$20 000 g mol^{-1}) and different molecular weight with constant AN content (F_{AN}) of 0.144 (see Table 1). A statistical copolymerization takes place given that acrylonitrile and acrylamide have similar Q and e values.[21] The structures of the obtained copolymers were confirmed by NMR (shown in Fig. S2 (ESI†)) and ATR-FTIR measurements (shown in Fig. S4 (ESI†)). Molecular weight and molecular weight distribution were determined by gel permeation chromatography (GPC) (Fig. S3 (ESI†)). Copolymer with F_{AN} = 0.042 was soluble in water and did not show any phase transition, *i.e.* appearing transparent at both lower and higher temperatures. Copolymer with F_{AN} = 0.262 was insoluble in water even when subjected to high temperatures (90 °C) for a longer period of time (8 hours) with or without sonication. Copolymers with F_{AN} from 0.086 to 0.221 exhibited UCST behaviour, *i.e.* displaying turbidity at lower temperatures and becoming transparent at higher temperatures (see Fig. 1). The summary of the visual observations of the solubility/phase behaviour of the copolymers in water is presented in Table 1. The visual observation confirmed that copolymers composed of hydrophilic acrylamide and ''hydroneutral'' acrylonitrile can show a UCST-type phase transition in water. It is well known that polyacrylamide forms intra and intermolecular hydrogen bonds in aqueous solution.[37,38] However, the homopolymer of polyacrylamide does not show a UCST due to its high hydrophilicity. On the other hand, poly(acrylonitrile) is insoluble in water. The insolubility of poly(acrylonitrile) in water strongly suggests that the –CN group has a low hydration number. Therefore the nitrile groups despite being polar should be considered as ''hydroneutral''; ''hydroneutral'' groups are defined as those functional groups displaying hydrophilicities intermediate between those of hydrophilic and hydrophobic groups with an hydration number close to 0.[39] However, the nitrogen atom of the –CN group can act as a proton acceptor for hydrogen bond formation with water molecules because of the presence of a lone-pair electron orbital. The –CN group has thus the capacity to form weak hydrogen bonds with water molecules but these bonds have lifetimes or interaction times close to or shorter than the rotational relaxation time of free water molecules.[39] The synergy of acrylamide and acrylonitrile contribute to the UCST behaviour of poly(AAm-*co*-AN) copolymer. Turbidimetry, SLS, DLS and SANS measurements were performed to study the phase transition and aggregation behaviour of poly(AAm-*co*-AN) copolymer solution as a function of AN contents, concentrations, as well as addition of electrolyte. For the DLS data, the cloud point temperature (T_{CP}) was determined from the minimum of the first derivative of the DLS curves (Fig. S5 (ESI†)) and for turbidimetry measurements, the cloud point temperature was taken as the initial turn point from the cooling cycle and final turn point from the heating cycle in the obtained transmittance *versus* temperature curves.

Table 1 Summary of the characteristics of poly(AAm-*co*-AN) copolymers with various AN fractions and their behaviour in water

No.	AN fraction in feed (f_{AN})	AN fraction in copolymer (F_{AN})	M_w[a] (kDa)	PDI	Phase behaviour in water[b]	T_{CP} [°C] at 1 mg mL^{-1} [c]
P1	0.100	0.042	18.1	1.26	Soluble	—
P2	0.145	0.086	18.3	1.29	UCST	5.5
P3	0.185	0.110	19.1	1.37	UCST	16.1
P4	0.225	0.144	20.2	1.27	UCST	29.9
P5	0.225	0.150	28.3	1.31	UCST	36.2[d]
P6	0.225	0.139	11.4	1.34	UCST	26.3[d]
P7	0.250	0.197	21.3	1.24	UCST	45.8
P8	0.275	0.221	18.5	1.42	UCST	56.5
P9	0.320	0.262	22.6	1.58	Insoluble	—

[a] Determined by GPC measurements. [b] Visual observation during heating and cooling. [c] Measured by turbidimetry. [d] c = 5 mg mL^{-1}.

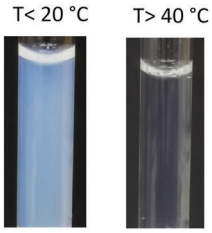

Fig. 1 Visual observation of poly(AAm-*co*-AN) copolymer in pure water (sample P4, F_{AN} = 0.144) at lower (T < 20 °C) and higher (T > 40 °C) temperatures.

3.2 Effect of AN content on phase transition and aggregation behaviour

At concentration of 1 mg mL^{-1} it can be observed from the turbidimetry measurements that the phase transition temperature of the copolymer increases with increasing AN fraction in the copolymer (Fig. 2a): the T_{CP} was found to be 5.5, 16.1, 25.9, 45.8 and 56.5 °C, for F_{AN} of 0.086, 0.11, 0.144, 0.197 and 0.221 respectively. At the same concentration of 1 mg mL^{-1}, the calculated phase transition temperature *via* DLS were 8, 17, 23, 44 and 57 °C (Fig. 2b) with hysteresis of 1–2 °C for the F_{AN} of 0.086, 0.11, 0.144, 0.197 and 0.221, respectively. The obtained T_{CP} from turbidimetry and from DLS measurements are plotted in Fig. 3. There is on average ±3 °C difference in the T_{CP} obtained by DLS as compared to turbidimetry measurement, which can be due to the different heating rate and data analysis. The obtained T_{CP} plot confirms a linear increase of phase transition temperature of the poly(AAm-*co*-AN) with increasing AN fraction in the copolymer. These results are expected, since increasing the fraction of hydroneutral acrylonitrile groups in the copolymer chain reduces the polymer–solvent interactions, *i.e.* increases the polymer–polymer interactions, thereby resulting in a shift of the phase transition temperature to higher temperatures (more energy needed to break the polymer–polymer interactions).

Below the phase transition temperature of the studied copolymers the hydrodynamic radius (R_h) of the copolymer was found to remain constant in the collapsed state for a given AN fraction: 37, 47, 63, 155 and 241 nm for the sample F_{AN} of 0.086, 0.11, 0.144, 0.197 and 0.221, respectively (Table 2), indicating the formation of larger aggregates with increasing

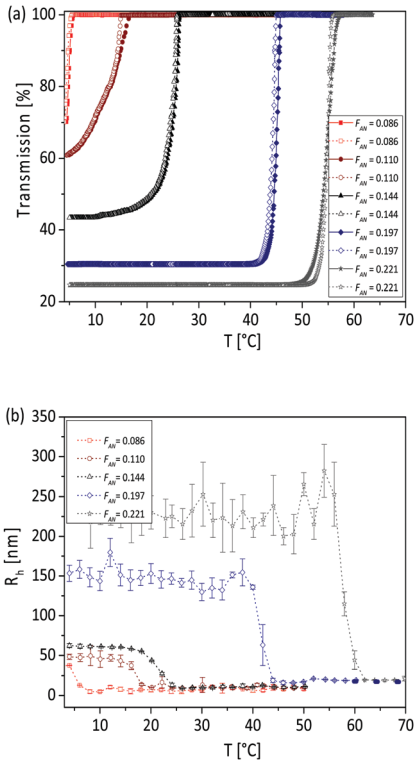

Fig. 2 (a) Turbidity curves of poly(AAm-*co*-AN) with various AN fractions in pure water at constant concentration of 1 mg mL^{-1} in heating and cooling cycle (b) hydrodynamic radius (R_h) *versus* temperature (T) curves in cooling cycle as a function of AN fraction in the copolymer at a concentration of 1 mg mL^{-1} in pure water. The filled symbol with solid line represents heating cycle and open symbol with dotted line represents cooling cycle.

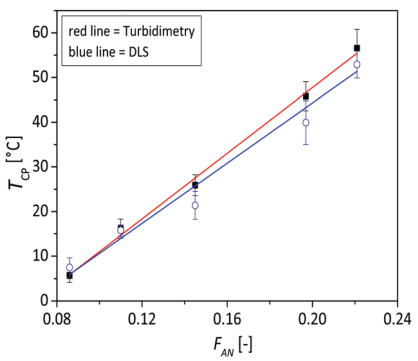

Fig. 3 T_{CP} obtained from turbidimetry and from DLS measurements are plotted against acrylonitrile fraction in the copolymer (F_{AN}). The red and blue solid lines are the linear fits of the obtained data from the turbidimetry and DLS measurements, respectively.

AN fraction in the copolymer. These results were consistent with the turbidimetry measurements (see Fig. 2a), where the turbidity increased in the collapsed state with increasing F_{AN} in the copolymer. Turbidity is the interaction between light and suspended particles in solution. The way in which the sample containing suspended particles interferes with transmittance light is related to the size, shape and composition of the particles and to the wavelength of the incident light.[40]

Table 2 Obtained average R_h value from DLS measurements below and above the phase transition temperature of poly(AAm-*co*-AN) with fixed concentration of 1 mg mL^{-1}

F_{AN}	R_h [nm] at 3 °C	R_h [nm] at 60 °C
0.086	37	5
0.110	47	10
0.144	63	13
0.197	155	17
0.221	241	20

With higher acrylonitrile content in the copolymer, the copolymer chains further minimize their interaction with water, resulting in more copolymer chains aggregating to form larger aggregates. Such stable aggregates (without using stabilizing agent), or so-called mesoglobules, can be formed by thermo-responsive polymers in the collapsed state as reported by Tenhu and co-workers.[41]

Above the phase transition temperature of the samples, where the copolymer chains are expanded and hydrated in water, the R_h was found to be of 5, 10, 13, 17 and 20 nm for the F_{AN} of 0.086, 0.11, 0.144, 0.197 and 0.221 respectively (Table 2), indicating a weak association between the copolymer chains. These are usually considered as "small associations" rather than unimers of copolymer chains,[42] most probably *via* the acrylamide units that are known to associate and form "multimacroion domains" when dissolved in water.[43] Such association of copolymer chains in the hydrated state was also observed in the literature.[44,45]

In order to get insights into the nature of the aggregates, we performed SLS measurements as a function of temperature. Fig. 4a shows the corresponding $Kc/R(\theta)$ *vs.* q^2 plot of poly(AAm-*co*-AN) (F_{AN} = 0.197) at a concentration of 1.3 mg mL^{-1} and selected temperatures from 15 to 55 °C. Below the phase transition temperature, a downward curves is observed and showed a linear relationship with q^2, indicating the presence of aggregates.[44] However, a downward curve is only observed at lower scattering angles above the phase transition temperature where small aggregates and unimers coexist. The apparent molecular weight ($M_{w,app}$) of the aggregates below T_{CP} and associated copolymer chains above T_{CP}, were calculated by extrapolation of q of the $Kc/R(\theta)$ *vs.* q^2 plot at lower scattering angles. The obtained $M_{w,app}$ is plotted as a function of temperature (Fig. 4b). Below 30 °C the $M_{w,app}$ is 140 times larger than the single polymer chain ($M_w \sim 2 \times 10^4$ g mol^{-1} from GPC) and remained constant, confirming the formation of stable mesoglobules. At $T \sim 30$ °C the $M_{w,app}$ decreased abruptly until a plateau was reached around 40 °C. In this plateau region the aggregation number was ~4–5, *i.e.* small aggregates in the collapsed state are present in solution. In addition, the radius of gyration (R_g) was determined as a function of temperature. The obtained R_g values are presented in the inset of Fig. 4b. The R_g remained constant at ~300 nm for $T < 30$ °C, then started to decrease and reached a plateau with a constant size of 40 nm in the collapsed state ($T > 40$ °C).

A detailed analysis of the association behaviour above the phase transition temperature was further done as a function of AN content with SLS measurements. Fig. 5 shows the corresponding

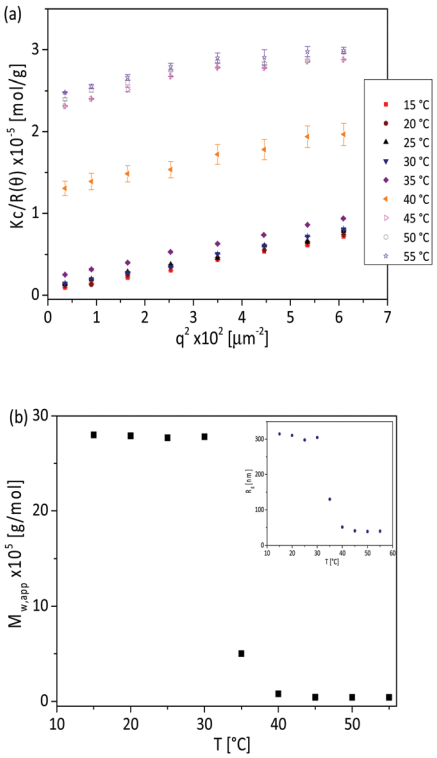

Fig. 4 (a) $Kc/R(\theta)$ *vs.* q^2 plot as a function of temperature at constant concentration of 1.3 mg mL^{-1} (F_{AN} = 0.197). (b) Calculated apparent molecular weight ($M_{w,app}$) as a function of temperature. The inset shows calculated radius of gyration as a function of temperature from 15 to 55 °C.

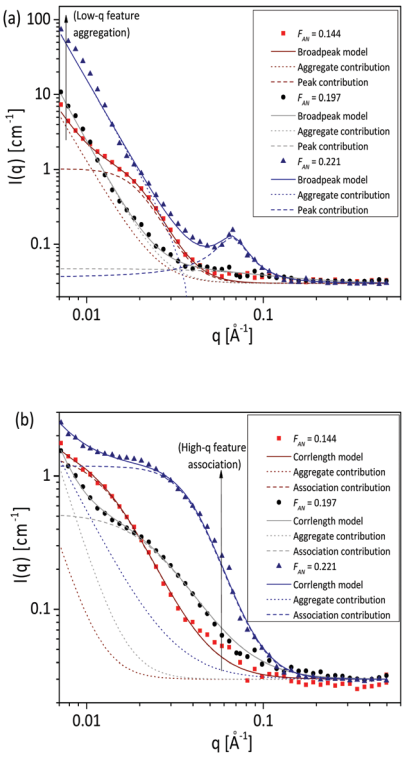

Fig. 6 SANS measurements of poly(AAm-*co*-AN) in D_2O at 25 °C (collapsed state) (a) and at 60 °C (soluble state) (b) with varying the acrylonitrile fractions (F_{AN}) from 0.144 to 0.221 and fixed concentration of 5 mg mL^{-1}. SANS data are fitted to the eqn (3). Individual contributions due to the aggregates and polymer chains interactions are shown with dashed lines.

$Kc/R(\theta)$ *vs.* q^2 plot of the poly(AAm-*co*-AN) solution (c = 5 mg mL^{-1}) at T = 55 °C. In this case the apparent molecular weight ($M_{w,app}$) of the associated chains was calculated by extrapolation in the lower q region of the $Kc/R(\theta)$ *vs.* q^2 plot. The obtained $M_{w,app}$ are shown in the inset of the Fig. 5. The $M_{w,app}$ is 23 times larger compared to the single polymer chain with increasing F_{AN} from 0.144 to 0.221. This confirmed the presence of small aggregates even above the phase transition temperature.

From the SANS measurements such aggregation and association behaviour below and above the phase transition temperature of poly(AAm-*co*-AN) can be confirmed. Fig. 6 shows the obtained results from SANS measurements. SANS curves for the samples with a polymer concentration of 5 mg mL^{-1} were fitted with an empirical formula of the form:

$$I(q) = \frac{A}{q^n} + \frac{C}{1 + (q\xi)^m} + B \qquad (3)$$

This model fits the total scattering as a sum of two separate effects plus an incoherent background B.[46] The first term is a power law decay describing the scattering from clusters or aggregates in the system, while the second term describes scattering from the polymer chains in solution. The size of the aggregates exceeds the measureable q range to be fully characterized, instead the degree of aggregation and surface structure can be determined from the scaling factor A and the exponent n respectively.

The length ξ is the correlation length of the polymer chains, while the exponent m is related to the excluded volume parameter of the polymer. The degree of aggregation in the system was determined by the relative magnitudes of the scaling factors A and C. A correlation peak for the sample with AN content 0.221 and 25 °C required modification of the fitting formula to take into account a peak at q_0:

$$I(q) = \frac{A}{q^n} + \frac{C}{1 + (|q - q_0|\xi)^m} + B \qquad (4)$$

The SANS results show significantly different scattering behaviour of the samples at 25 °C and 60 °C as expected. At 25 °C

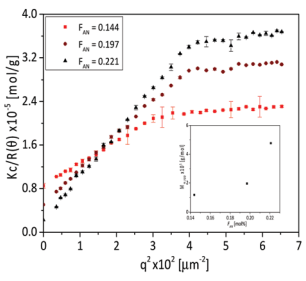

Fig. 5 $Kc/R(\theta)$ *vs.* q^2 plot of poly(AAm-*co*-AN) copolymer solutions with different AN contents at constant concentration of 5 mg mL^{-1} above the T_{CP}. The inset represents the calculated apparent molecular weight of the copolymers as a function of F_{AN}.

(below phase transition temperature of the copolymers), the scattering is dominated by the first term in eqn (3), showing that the systems have formed aggregates (see Fig. 6a). At 60 °C, the scattering from the polymer chains dominates the system. Small upturns at very low q suggest a small amount of clustering is present at these temperatures (see Fig. 6b).

The effect of AN content on the behaviour of the systems can be seen at both 25 °C and 60 °C. At 60 °C, increasing AN content shortens the correlation length of the polymer chains, from 75 Å at 0.144 AN fraction to 25 Å at F_{AN} 0.221, reflecting the increasing polymer–polymer interactions at higher AN contents. At 25 °C, increasing AN content increases the relative strength of the scattering contribution from the aggregates. At F_{AN} of 0.144, the scattering contribution from the polymer chains is visible in the high q region, with the aggregations increasing scattering intensity in the low q region to produce an upturn at low q. As the AN content is increased, the scattering from the aggregates increasingly dominates, with the power law decay due to aggregates increasing. At the highest AN content of 0.221, in addition to a power law decay, there is a correlation peak in the scattering at q_0 = 0.066 Å. This indicates there are large aggregates forming in the system, within which the polymer chains strongly interact, to produce a degree of ordering of the chains with a characteristic distance of 95 Å.

3.3 Effect of concentration on phase transition and aggregation behaviour

We investigated the phase transition and aggregation behaviour of poly(AAm-*co*-AN) copolymer solutions from diluted (1 mg mL^{-1}) to concentrated (50 mg mL^{-1}) conditions. Above the concentration of 50 mg mL^{-1} the copolymer solutions were not stable and precipitated after 3 to 4 h. The obtained concentration dependent turbidity curves and DLS measurements are shown in Fig. 7. From both measurements, it was observed that the phase transition temperature of poly(AAm-*co*-AN) varies, typically 10 °C over the measured concentration range. Concentration dependent phase transition temperature were also observed in the report of Hou *et al.*[28] and Seuring *et al.*[21] From the turbidimetry measurements, the T_{CP} was found around 5.5, 8, 10.6, 12.8, 14.5 and 16.6 °C for the concentration of 1, 5, 10, 20, 30 and 50 mg mL^{-1}, respectively (for the sample P2 where the AN fraction in the copolymer (F_{AN}) is 0.086). To confirm the results obtained from the turbidimetry measurements, DLS measurements were used as a complementary technique. The calculated T_{CP} were 6.1, 8.13, 10.3, 12.17, 14.09 and 16.14 for the concentration of 1, 5, 10, 20, 30 and 50 mg mL^{-1} respectively, which is in good agreement with the results found with the turbidimetry measurements. The obtained T_{CP} are plotted as a function of concentration in Fig. 8. The shape of the fitting curves indicates an exponential increase of the phase transition temperature with increasing concentration of poly(AAm-*co*-AN) solution. It is known that entanglement between the copolymer chains is favoured at higher concentration. Therefore, a network structure could form in the solutions that results in higher phase transition temperature. The influence of chain entanglement onto phase transition behaviour has also been observed previously.[47,48] This offers the possibility to fine tune the thermal response of a system by adjusting the concentration of the solutions.

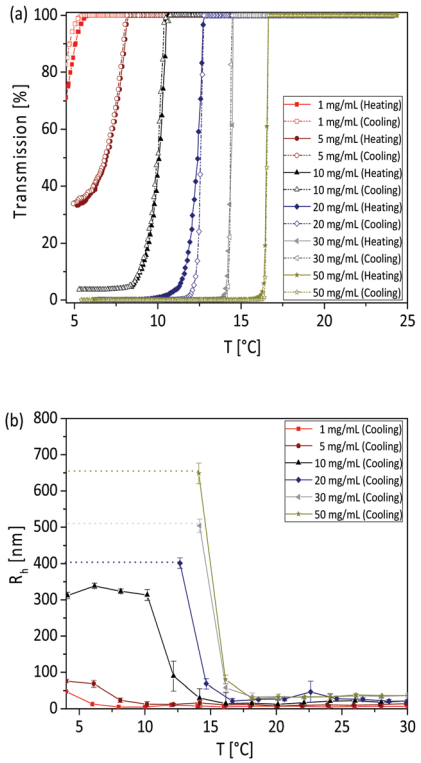

Fig. 7 (a) Turbidity curves of poly(AAm-*co*-AN) in water with various concentrations of the sample of F_{AN} = 0.086 in heating and cooling cycles (b) concentration dependent hydrodynamic radius (R_h) *versus* temperature (T) for sample F_{AN} = 0.086 in cooling cycle. The dotted line represents the constant R_h value below the phase transition temperature (assumed).

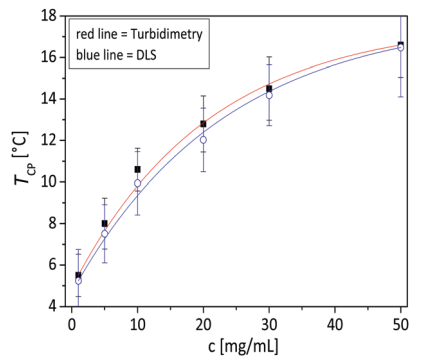

Fig. 8 T_{CP} from turbidimetry and DLS measurements are plotted against concentration of the poly(AAm-*co*-AN) copolymer solutions. The red and blue solid lines are the exponential fits of the obtained data from the turbidimetry and DLS measurements, respectively.

In the collapsed state, it can be seen that the transmission value increases upon dilution of the solution in the dilute regime (see turbidity curves in Fig. 7a). Moreover, the obtained average R_h values from DLS measurements, presented in Table 3, displayed a increase of R_h from 46 to 654 nm with raising the concentration from 1 to 50 mg mL^{-1} below the T_{CP} of the solutions. This result clearly indicates the formation of larger aggregates with increasing the concentration of the solutions.

Table 3 Obtained average R_h value from the DLS measurements below and above the phase transition temperature of poly(AAm-*co*-AN) with fixed acrylonitrile fraction (F_{AN} = 0.086)

Conc. [mg mL^{-1}]	R_h [nm] at 3 °C	R_h [nm] at 30 °C
1	46	5
5	76	14
10	329	19
20	404	21
30	512	32
50	654	37

In the report of Hou *et al.*[28] a similar trend was observed: the more concentrated the poly(AAm-*co*-AN) solution the larger the hydrodynamic diameter was. The larger aggregates formation can be explained in two ways: firstly, increasing concentration enhanced the formation of entanglement between the copolymer chains, leading to the formation of larger aggregates. Secondly, the higher concentrations weaken the hydrogen bonding between polymer chains and water molecules, and strengthen the intra/inter-chain hydrophobic interactions of the polymer leading to the formation of aggregates. It has been documented that the size of the mesoglobules formed in collapsed state increases with increasing the concentrations of the solution.[41,49]

Above the phase transition temperature of poly(AAm-*co*-AN), concentration dependent association behaviour was observed. The obtained R_h at 30 °C is shown in Table 3. The R_h for the normal polymer chains is usually smaller than 10 nm.[42,50] The R_h found in this study is around 5 to 37 nm, clearly showing an association between the copolymer chains, involving a small number of unimers (copolymer chains), even at temperatures above the phase transition.

The association between copolymer chains leading to the formation of smaller aggregates above the phase transition temperature were further examined by SLS measurements at different concentrations. Fig. 9 shows the $Kc/R(\theta)$ *vs.* q^2 plot of poly(AAm-*co*-AN) (F_{AN} = 0.086) at T = 30 °C. The $M_{w,app}$ was calculated by using eqn (2) and extrapolating the $q \rightarrow 0$ at lower region. The inset of Fig. 9 shows that the $M_{w,app}$ increased slowly with increasing concentration of the solutions at $c < 10$ mg mL^{-1}, then an abrupt increase of $M_{w,app}$ was observed with increasing concentrations for concentrations above 10 mg mL^{-1} (inset of Fig. 9).

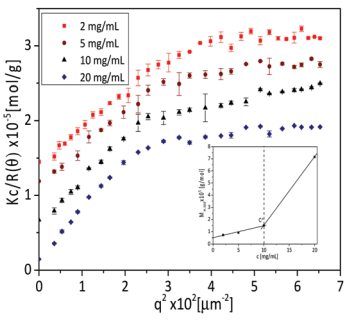

Fig. 9 $Kc/R(\theta)$ *vs.* q^2 plot for poly(AAm-*co*-AN) (F_{AN} = 0.086) in water at different concentrations above the phase transition temperature (T = 30 °C). The inset figure shows the concentration dependence of the apparent molecular weight ($M_{w,app}$) of associated chains.

The $M_{w,app}$ was 35 times larger compared to a single polymer chain ($M_w \sim 20\,000$ g mol^{-1} by GPC) for a concentration of 20 mg mL^{-1}.

According to the polymer solutions theory, it is possible to differentiate between the dilute and semidilute or concentrated states where the polymer coils overlap and interact. The change from isolated coils to overlapping ones can be characterized by the overlap concentration C^* given by:[51]

$$C^* = \frac{3M}{4\pi N_A R_g^3} \quad (5)$$

where M, R_g and N_A are the polymer molecular weight, radius of gyration of the polymer chain and the Avogadro's number, respectively. According to the Kirkwood–Risemann theory[52] the radius of gyration can be determined as $R_g = 3/2R_h$ in a good solvent. For the investigated copolymer (F_{AN} = 0.086, M_n = 14 200 g mol^{-1}) in the coil state (R_h = 5 nm, see Table 3), the R_g is estimated to be 7.5 nm according to the reference. C^* is 12.9 mg mL^{-1} using eqn (5). This determined overlap concentration is in agreement with the experimental concentration of ~10 mg mL^{-1}, where the apparent molecular weight abruptly increased (inset Fig. 9). In the condensed state different copolymer chains interpenetrate, which leads to the association between copolymer chains and the formation of aggregates.

SANS measurements for two different concentrations as presented in Fig. 10 also confirmed the results obtained from

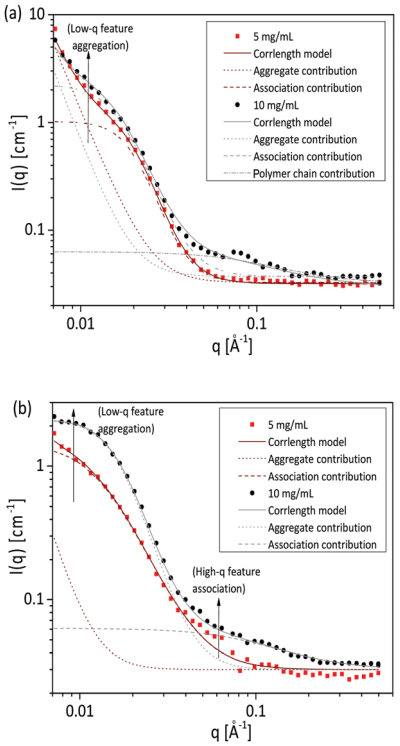

Fig. 10 SANS measurements of poly(acrylamide-*co*-acrylonitrile) copolymer in D_2O at 25 °C (collapsed state) (a) and at 60 °C (soluble state) (b) with varying concentration at fixed acrylonitrile fraction (F_{AN}) of 0.144. SANS data are fitted to the eqn (3) and also the association contribution and polymer chain contribution is included.

turbidimetry, SLS and DLS measurements. The sample with 0.144 AN fraction was measured at 5 mg mL^{-1} and 10 mg mL^{-1} polymer concentration. At higher concentration, an additional Lorentzian term with scaling factor D provides an average description of the scattering curves in the medium q region:

$$I(q) = \frac{A}{q^n} + \frac{C}{1+(q\xi)^m} + \frac{D}{1+(q\xi)^2} + B \qquad (6)$$

For both concentrations at 25 °C, the same scattering behaviour in the medium q region was observed. The presence of aggregates can be seen from the upturn at low q due to power law decay. Fig. 10a shows that the aggregates are concentration dependent where the aggregate contribution increases with increasing concentration of the solutions. While at 60 °C, an increase in the polymer concentration from 5 mg mL^{-1} to 10 mg mL^{-1} causes the aggregate contribution to vanish, and the correlation length to decrease from 75 to 62 Å. It can be observed in Fig. 10b that the association contribution, which is observed at high-q value, is enhanced by the higher polymer concentration.

3.4 Effect of copolymer chain length on the UCST behaviour

The effect of the copolymer chain length on the UCST of poly(AAm-*co*-AN) was studied at a fixed AN fraction (F_{AN} = 0.144) and concentration of the solution (5 mg mL^{-1}). As can be seen from the turbidity curves (Fig. 11), the phase transition temperature is shifted to higher temperatures with increasing copolymer chain length. The phase transition temperature increased around 10 °C by increasing molecular weight from 11.4 to 28.3 kDa. By increasing the copolymer molecular weight, the overall amount of acrylonitrile groups increases in the copolymer chains. These acrylonitrile groups enhance the polymer–polymer interactions. Therefore, higher temperatures are needed to reduce these polymer–polymer interactions. Such behaviour is also observed for LCST polymers. The LCST is expected to decrease with increasing molecular weight based on the changes in the polymer–solvent interactions.[53,54] It is also well known that the LCSTs of PNIPAM can be decreased by the presence of hydrophobic end groups and increased by hydrophilic end groups.[55]

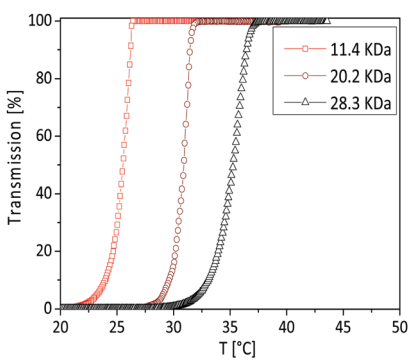

Fig. 11 Turbidity curves of the poly(AAm-*co*-AN) in water by varying the copolymer chain length in cooling cycle. The concentration of the solution is 5 mg mL^{-1}.

3.5 Effect of electrolyte on phase transition and aggregation behaviour

The phase transition and aggregation behaviour of poly(AAm-*co*-AN) solution at fixed acrylonitrile fraction (F_{AN}) of 0.144 was studied as a function of different types of electrolytes (NaSCN, NaCl and Na_2SO_4) and electrolyte concentrations (50, 100, 200 and 300 mM). Since the cation (Na^+) was kept constant in this study while the anion was varied, the influence of the latest on the phase transition temperature of poly(AAm-*co*-AN) was determined. The obtained results from the turbidimetry measurements are presented in Fig. 12. NaCl has a minimal influence on the phase transition temperature of copolymer solution (30 °C in pure water). The phase transition temperature slightly increased below 50 mM of NaCl and then decreased to 20 °C by the addition of 300 mM NaCl. This tendency was previously observed by Hou *et al.*[28] who found that the phase transition temperature of poly(AAm-*co*-AN) decreased of about 5 °C upon addition of 150 mM NaCl.[56] The effect of NaCl on poly(AAm-*co*-AN) is comparable to that of UCST type PNAGA system. Liu *et al.*[57] observed that the phase transition temperature of non-ionic PNAGA increases with addition of small amount of NaCl. Nevertheless, the phase transition temperature steadily decreased with further addition of NaCl and the phase transition temperature disappeared with the addition of around 1000 mM of NaCl. This behaviour is also typically observed in LCST polymers like PNIPAM, and in such cases the effect can be explained by intra and intermoleculer effect.[58–61] The addition of 300 mM "chaotropic" NaSCN salt (the terms "chaotrope" and "kosmotrope" refer to the classification of salts according to the Hofmeister series;[62] chaotropic agents increase the hydrophobic effects within the solution, while kosmotropic agents contribute to the stability and structure of water–water interactions) leads to a significant decrease of the phase transition temperature from 30 to 12 °C. The decrease of the phase transition temperature by addition of NaSCN and NaCl can occur due to polarization effects, surface tension, as well as direct ion binding. The "kosmotropic" Na_2SO_4 salt showed the most pronounced effect on the phase transition temperature of

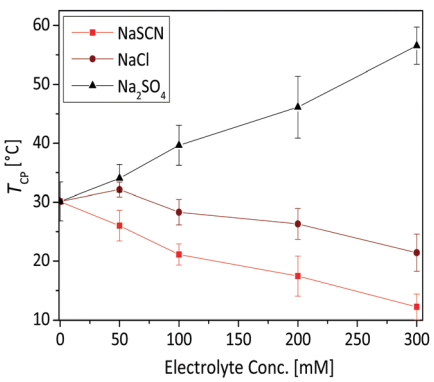

Fig. 12 T_{CP} temperature of poly(AAm-*co*-AN) at fixed acrylonitrile fraction (F_{AN}) of 0.144 against electrolyte concentration is plotted. The copolymer concentration was 5 mg mL^{-1} using different salts (NaSCN, NaCl and Na_2SO_4). The data were taken during the cooling cycle of the measurements.

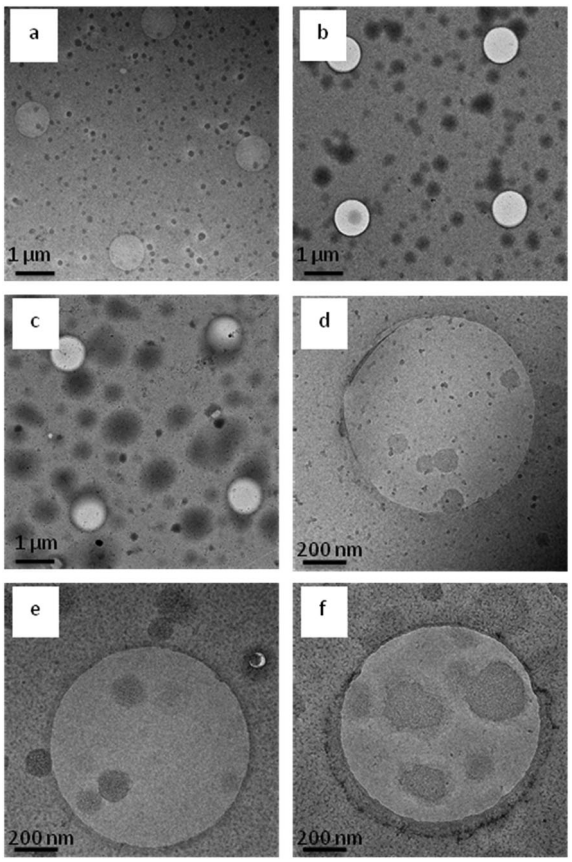

Fig. 13 Cryo-TEM measurements of the poly(AAm-*co*-AN) copolymer solution at 25 °C. Images of (a) (F_{AN} = 0.144), (b) (F_{AN} = 0.197) and (c) (F_{AN} = 0.221) represent the acrylonitrile effect on the aggregate size with fixed concentration of 5 mg mL^{-1}. Images of (d) (1 mg mL^{-1}), (e) (5 mg mL^{-1}) and (f) (10 mg mL^{-1}) representing concentration effect on the aggregate size with fixed acrylonitrile fraction (F_{AN} = 0.144).

poly(AAm-*co*-AN). In this case the phase transition temperature increased from 30 to 56 °C by addition of 300 mM Na_2SO_4 to the solution. This effect was expected as when more ions are present in the solution they interfere with the hydrogen bonding between H_2O molecules and copolymer chains disrupting the regular hydration shell around the temperature sensitive polymer chains. Therefore interchain and intrachain hydrophobic effects among the polymer chains are favoured, which increases the phase transition temperature of the poly(AAm-*co*-AN).

In order to better understand the structures of the formed aggregates and correlate them with the data obtained from DLS, turbidimetry and SANS measurements, the systems were visualized by cryo-TEM measurements (see Fig. 13). Cryo-TEM measurements were obtained from pure water solution of poly(AAm-*co*-AN) with different AN fractions and concentrations of the solutions. We observed that the formed mesoglobules are spherical in shape and their size increases with increasing AN fractions and concentrations of the solutions as found by the other techniques.

Fig. 14 represents the proposed model for the temperature-induced aggregation and association behaviour of the poly(AAm-*co*-AN) in pure water. By varying the composition and concentration,

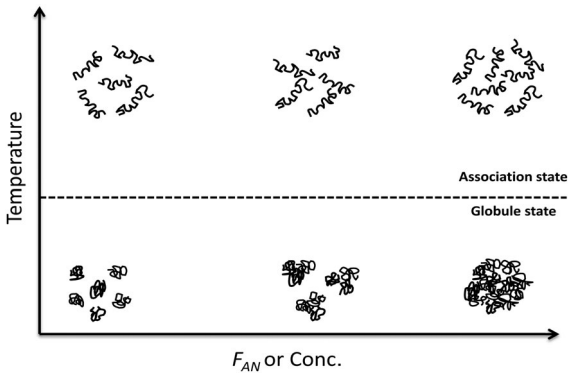

Fig. 14 Schematic illustration of the proposed temperature-induced aggregation behaviour of the poly(AAm-*co*-AN) in aqueous solution as a function of the acrylonitrile contents (F_{AN}) and the concentrations of the solutions.

various aggregation behaviour of poly(AAm-*co*-AN) were observed by turbidimetry, SLS, DLS and SANS measurements. The increasing amount of AN contents in the copolymers resulted in stronger hydrophobic interactions between copolymer chains which lead to the formation of larger aggregates in the dehydrated state of poly(AAm-*co*-AN). While in the hydrated state, the hydroneutral part of the chains (acrylonitrile in the copolymers) plays a role in the association, that results in a weak association, *i.e.* small aggregates, in the soluble state.

4 Conclusions

In this report, a robust UCST-type poly(AAm-*co*-AN) copolymer with different compositions was prepared through RAFT polymerization. The temperature-induced phase transition and the aggregation behaviour of the poly(AAm-*co*-AN) were studied according to different AN contents in the copolymer, various concentrations of the copolymer solutions and copolymer chain lengths in pure water. The addition of electrolyte to the system was also investigated. The temperature-induced phase transition and aggregation behaviour was systematically studied by a combination of turbidimetry, static and dynamic light scattering, SANS measurements and cryo-TEM. We found that the phase transition temperature is composition dependent: the phase transition temperature increases with increasing acrylonitrile content in the copolymers. From the DLS measurements it was shown that the poly(AAm-*co*-AN) chains are hydrated (coil) above the phase transition temperature and are present either as unimers or small aggregates composed of few polymeric chains (R_h less than 40 nm) depending on the AN content in the copolymer. Upon cooling the hydrodynamic radii increased (up to few hundreds of nm), indicating the formation of larger aggregates. The size of the aggregates was found to increase with increasing acrylonitrile content in the copolymer, as confirmed by static and dynamic light scattering, SANS and cryo-TEM measurements. In addition, the phase transition temperature and aggregation behaviour strongly depend on the solution concentration. The phase transition temperature decreased upon dilution of the copolymer solutions. The aggregate size

was found to increase with increasing solution concentrations below phase transition temperature, indicating the formation of larger aggregates. Furthermore, the phase transition temperature can be tuned by addition of electrolyte into the solutions or by varying the copolymer chain length.

Acknowledgements

We would like to thank Marlies Gräwert (Max Planck Institute of Colloids and Interfaces, Potsdam-Golm, Germany) for the GPC measurements. We are grateful to Dr. Christoph Böttcher as well as Dr. Boris Schade (Freie Universität Berlin, Germany) for the cryo-TEM measurements. We are grateful to the group of Prof. Helmut Schlaad (University of Potsdam, Germany) for the opportunity to use their turbidimetry spectrometer. We also would like to thank Frank Milczewski for the ATR-FTIR measurements. We also thank HZB for the allocation of neutron beamtime. Funding by the BAM-MIS program is acknowledged.

References

1 M. R. Aguilar and J. S. Roman, *Smart polymers and their applications, part I: Types of smart polymer*, Woodhead Publishing, Cambridge, UK, 1st edn, 2014.
2 G. Pan, Q. Guo, C. Cao, H. Yang and B. Li, *Soft Matter*, 2013, **9**, 3840–3850.
3 D. Roy, W. L. A. Brooks and B. S. Sumerlin, *Chem. Soc. Rev.*, 2013, **42**, 7214–7243.
4 C. Scholz and J. Kressler, *Tailored polymer architectures for pharmaceutical and biomedical applications*, Oxford University Press, Oxford, UK, 2013.
5 D. Schmaljohann, *Adv. Drug Delivery Rev.*, 2006, **58**, 1655–1670.
6 M. Füllbrandt, E. Ermilova, A. Asadujjaman, R. Hölzel, F. F. Bier, R. von Klitzing and A. Schönhals, *J. Phys. Chem. B*, 2014, **118**, 3750–3759.
7 M. Dan, Y. Su, X. Xiao, S. Li and W. Zhang, *Macromolecules*, 2013, **46**, 3137–3146.
8 E. A. Clark and J. E. G. Lipson, *Polymer*, 2012, **53**, 536–545.
9 V. Aseyev, H. Tenhu and F. Winnik, *Adv. Polym. Sci.*, 2011, **242**, 29–89.
10 J. Seuring and S. Agarwal, *Macromol. Rapid Commun.*, 2012, **33**, 1898–1920.
11 J. Seuring and S. Agarwal, *ACS Macro Lett.*, 2013, **2**, 597–600.
12 Z. Zhang, T. Chao, S. Chen and S. Jiang, *Langmuir*, 2006, **22**, 10072–10077.
13 V. Mishra, S.-H. Jung, H. M. Jeong and H.-i. Lee, *Polym. Chem.*, 2014, **5**, 2411–2416.
14 A. Fujihara, N. Shimada, A. Maruyama, K. Ishihara, K. Nakai and S.-i. Yusa, *Soft Matter*, 2015, **11**, 5204–5213.
15 Q. Zhang and R. Hoogenboom, *Chem. Commun.*, 2015, **51**, 70–73.
16 J. Niskanen and H. Tenhu, *Polym. Chem.*, 2016, DOI: 10.1039/C6PY01612J.
17 H. C. Haas and N. W. Schuler, *J. Polym. Sci., Part B: Polym. Lett.*, 1964, **2**, 1095–1096.
18 N. M. Brahme and W. T. Smith, *J. Polym. Sci., Polym. Chem. Ed.*, 1984, **22**, 813–820.
19 J. Seuring, F. M. Bayer, K. Huber and S. Agarwal, *Macromolecules*, 2012, **45**, 374–384.
20 F. Liu, J. Seuring and S. Agarwal, *Polym. Chem.*, 2013, **4**, 3123–3131.
21 J. Seuring and S. Agarwal, *Macromolecules*, 2012, **45**, 3910–3918.
22 C. Echeverria, D. López and C. Mijangos, *Macromolecules*, 2009, **42**, 9118–9123.
23 H. Katono, A. Maruyama, K. Sanui, N. Ogata, T. Okano and Y. Sakurai, *J. Controlled Release*, 1991, **16**, 215–227.
24 P. Bouillot and B. Vincent, *Colloid Polym. Sci.*, 2000, **278**, 74–79.
25 F. Liu, S. Jiang, L. Ionov and S. Agarwal, *Polym. Chem.*, 2015, **6**, 2769–2776.
26 G. Huang, H. Li, S.-T. Feng, X. Li, G. Tong, J. Liu, C. Quan, Q. Jiang, C. Zhang and Z. Li, *Macromol. Chem. Phys.*, 2015, **216**, 1014–1023.
27 B. A. Pineda-Contreras, H. Schmalz and S. Agarwal, *Polym. Chem.*, 2016, **7**, 1979–1986.
28 L. Hou and P. Wu, *Soft Matter*, 2015, **11**, 7059–7065.
29 H. Zhang, S. Guo, W. Fan and Y. Zhao, *Macromolecules*, 2016, **49**, 1424–1433.
30 H. Zhang, X. Tong and Y. Zhao, *Langmuir*, 2014, **30**, 11433–11441.
31 F. Käfer, F. Liu, U. Stahlschmidt, V. Jérôme, R. Freitag, M. Karg and S. Agarwal, *Langmuir*, 2015, **31**, 8940–8946.
32 S. Mitragotri and J. Lahann, *Nat. Mater.*, 2009, **8**, 15–23.
33 M. I. Tiwana, S. J. Redmond and N. H. Lovell, *Sens. Actuators, A*, 2012, **179**, 17–31.
34 B. J. Frisken, *Appl. Opt.*, 2001, **40**, 4087–4091.
35 B. H. Zimm, *J. Chem. Phys.*, 1945, **13**, 141–145.
36 K. Vogtt, M. Siebenburger, D. Clemens, C. Rabe, P. Lindner, M. Russina, M. Fromme, F. Mezei and M. Ballauff, *J. Appl. Crystallogr.*, 2014, **47**, 237–244.
37 F. A. Bovey and G. V. D. Tiers, *J. Polym. Sci., Part A: Gen. Pap.*, 1963, **1**, 849–861.
38 N. Tanaka, K. Ito and H. Kitano, *Macromolecules*, 1994, **27**, 540–544.
39 N. Sagawa and T. Shikata, *Phys. Chem. Chem. Phys.*, 2014, **16**, 13262–13270.
40 M. M. A. Elsayed and G. Cevc, *Pharm. Res.*, 2011, **28**, 2204–2222.
41 V. Aseyev, S. Hietala, A. Laukkanen, M. Nuopponen, O. Confortini, F. E. Du Prez and H. Tenhu, *Polymer*, 2005, **46**, 7118–7131.
42 S. Sun, P. Wu, W. Zhang, W. Zhang and X. Zhu, *Soft Matter*, 2013, **9**, 1807–1816.
43 L. Deng, C. Wang, Z.-C. Li and D. Liang, *Macromolecules*, 2010, **43**, 3004–3010.
44 J. Yan, W. Ji, E. Chen, Z. Li and D. Liang, *Macromolecules*, 2008, **41**, 4908–4913.
45 J. V. M. Weaver, I. Bannister, K. L. Robinson, X. Bories-Azeau, S. P. Armes, M. Smallridge and P. McKenna, *Macromolecules*, 2004, **37**, 2395–2403.
46 B. Hammouda, D. L. Ho and S. Kline, *Macromolecules*, 2004, **37**, 6932–6937.

47 Y. Lin, Y.-g. Shangguan, B.-w. Qiu, W.-w. Yu, F. Chen, Z.-w. Guo and Q. Zheng, *Chin. J. Polym. Sci.*, 2015, **33**, 869–879.
48 K. Yang, Y. Z. Yang, C. L. Hu, Y. Y. Huang, W. K. Zhang, X. D. Chen and M. Q. Zhang, *Macromol. Chem. Phys.*, 2012, **213**, 1735–1741.
49 A. V. Gorelov, A. Du Chesne and K. A. Dawson, *Phys. A*, 1997, **240**, 443–452.
50 P. J. Roth, T. P. Davis and A. B. Lowe, *Macromolecules*, 2012, **45**, 3221–3230.
51 P.-G. Gennes, *Scaling Concepts in Polymer Physics*, Cornell University Press, Ithaca, New York, 1979.
52 J. G. Kirkwood and J. Riseman, *J. Chem. Phys.*, 1948, **16**, 565–573.
53 D. Patterson, *Macromolecules*, 1969, **2**, 672–677.
54 D. G. Lessard, M. Ousalem and X. X. Zhu, *Can. J. Chem.*, 2001, **79**, 1870–1874.
55 Y. Xia, X. Yin, N. A. D. Burke and H. D. H. Stöver, *Macromolecules*, 2005, **38**, 5937–5943.
56 V. Hildebrand, A. Laschewsky and D. Zehm, *J. Biomater. Sci., Polym. Ed.*, 2014, **25**, 1602–1618.
57 F. Liu, J. Seuring and S. Agarwal, *J. Polym. Sci., Part A: Polym. Chem.*, 2012, **50**, 4920–4928.
58 L. Lu, Z. Wang and Y. Cao, *J. Wuhan Univ. Technol., Mater. Sci. Ed.*, 2012, **27**, 285–289.
59 T. Liu, J. Fang, Y. Zhang and Z. Zeng, *Macromol. Res.*, 2008, **16**, 670–675.
60 X.-M. Liu, K. P. Pramoda, Y.-Y. Yang, S. Y. Chow and C. He, *Biomaterials*, 2004, **25**, 2619–2628.
61 F. Garret-Flaudy and R. Freitag, *J. Polym. Sci., Part A: Polym. Chem.*, 2000, **38**, 4218–4229.
62 F. Hofmeister, *Arch. Exp. Pathol. Pharmakol.*, 1888, **24**, 247–260.